Supporting Information

Size-dependence on Electrochemical Performance of Fe-N-C Catalysts for Oxygen Reduction and Cathodes of Direct Methanol Fuel Cells

Xinlong Xu, [a, b] Zhangxun Xia, [a] Xiaoming Zhang, [a] Huanqiao Li, [a] Suli Wang, *[a] Gongquan Sun*[a]

[a] Division of Fuel Cell & Battery, Dalian National Laboratory for Clean Energy, Dalian Institute of Chemical Physics, Chinese Academy of Sciences, Dalian 116023, China

[b] University of Chinese Academy of Sciences, Beijing 100049, China

1. Figure S1-S14

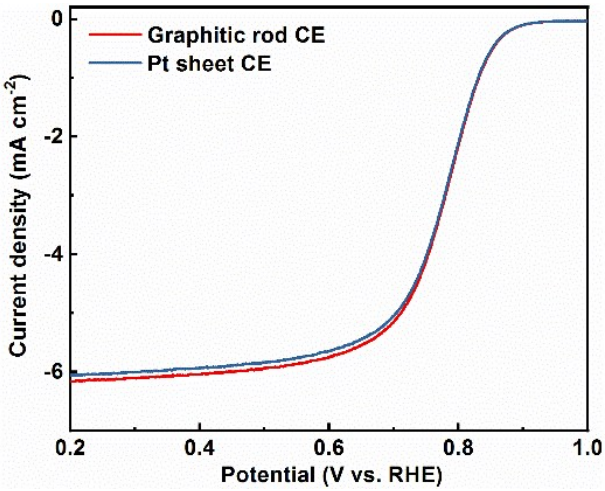

Figure S1. Comparison of LSV curves tested with Pt and graphite counter electrodes.

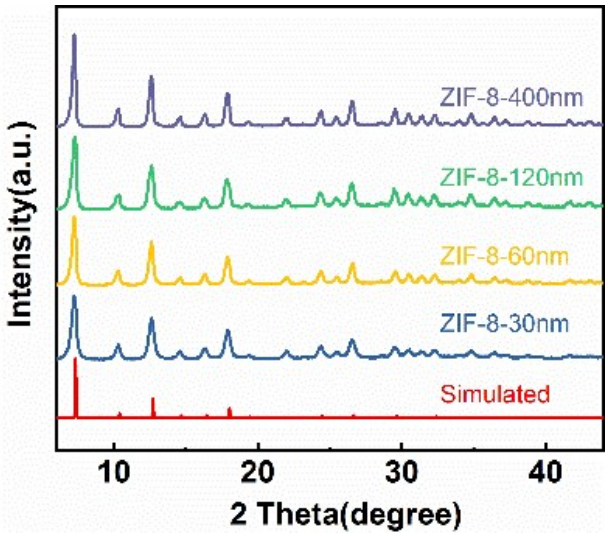

Figure S2. XRD of ZIF-8 with different sizes.

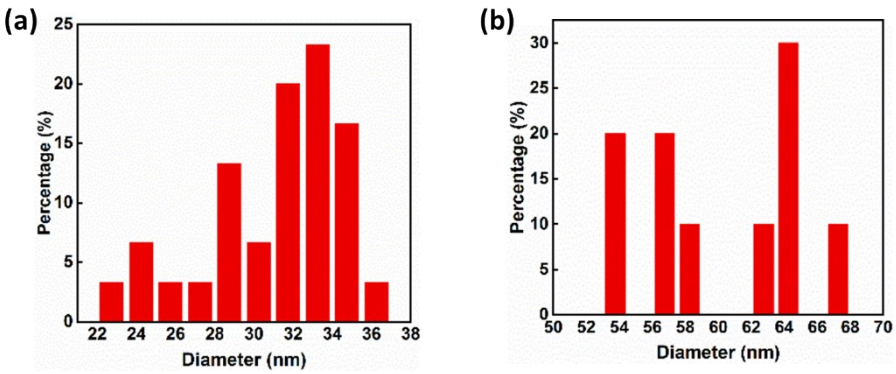

Figure S3. The size distribution of ZIF-8-30 and ZIF-8-60. The sizes are given in the form of statistical results because of the large number of particles under TEM.

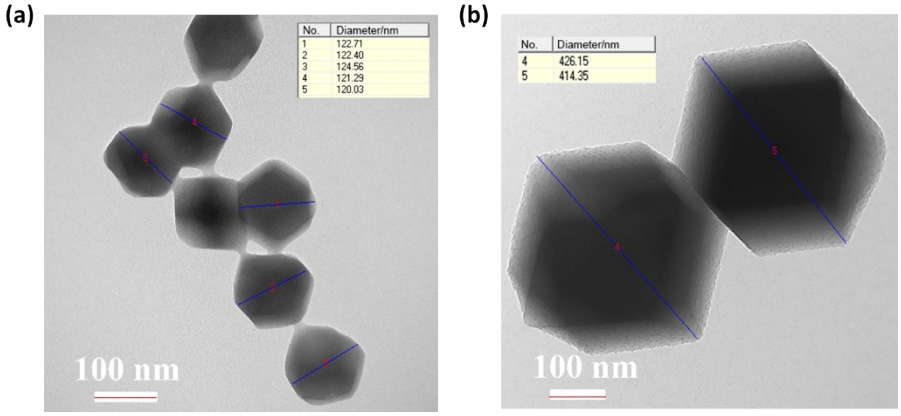

Figure S4. The size distribution of ZIF-8-120 and ZIF-8-400. The sizes are present directly because of the small number of particles under TEM.

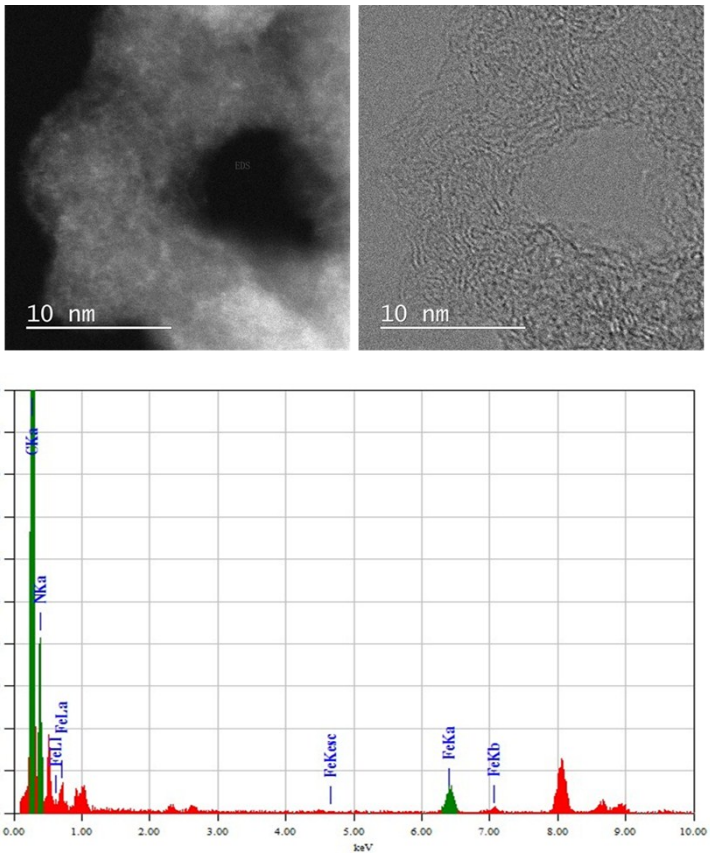

Figure S5. The STEM images of Fe-N-C-30 and the corresponding EDS.

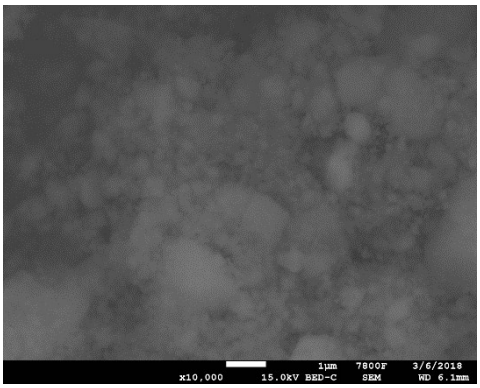

Figure S6. The BSE-SEM image of Fe-N-C-30. The agglomeration of Fe is still invisible under a large area of view (100 μm2), ensuring that Fe is present in the catalyst as FeNx.

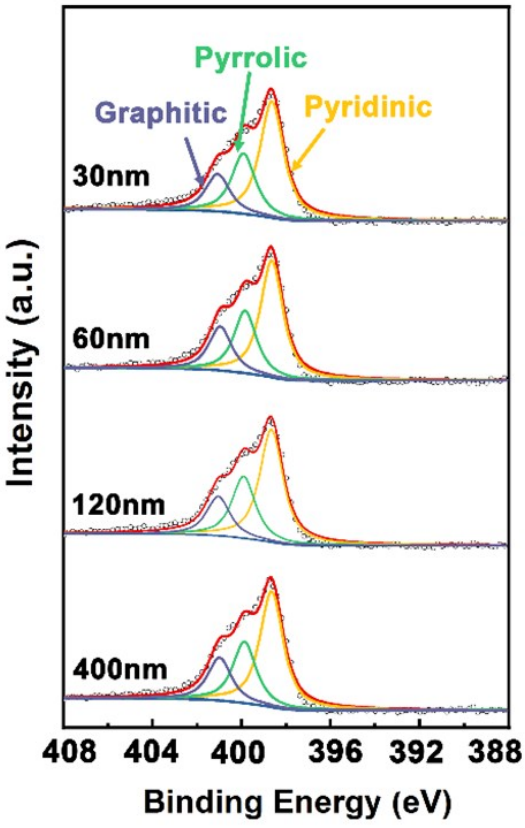

Figure S7. High-resolution N1s spectrums of Fe-N-C with different sizes.

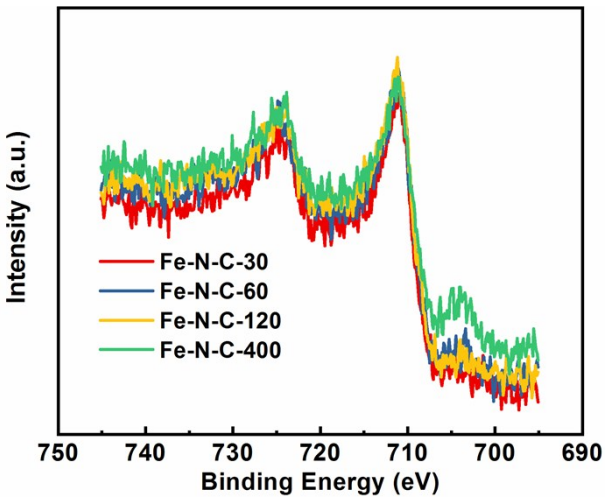

Figure S8. High-resolution Fe2p spectrums of Fe-N-C with different sizes.

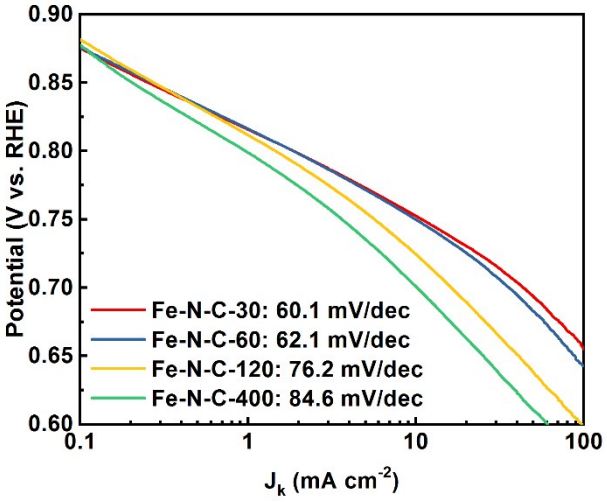

Figure S9. Tafel plots of Fe-N-C with different sizes.

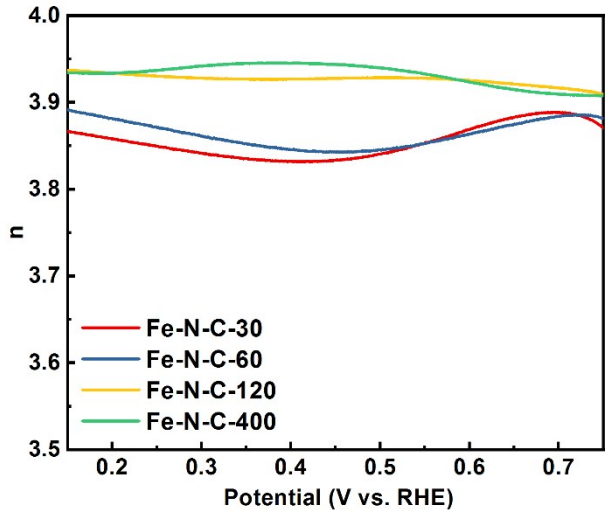

Figure S10. The electron transfer number calculated from RRDE results.

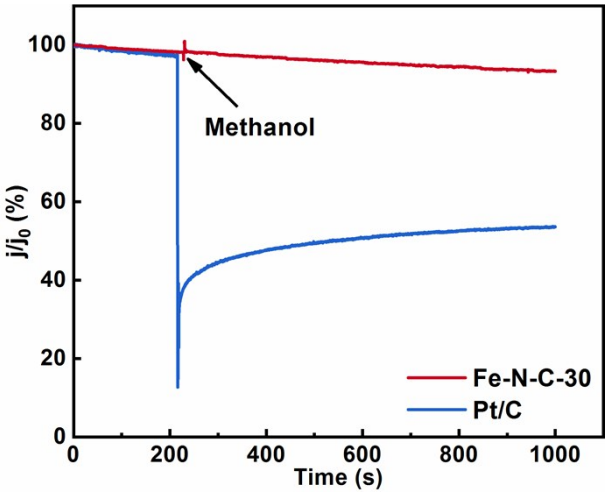

Figure S11. Chronoamperometric response of Fe-N-C-30 and commercial 20 wt% Pt/C at 0.7 V with the addition of methanol (0.5 M) at 200 s.

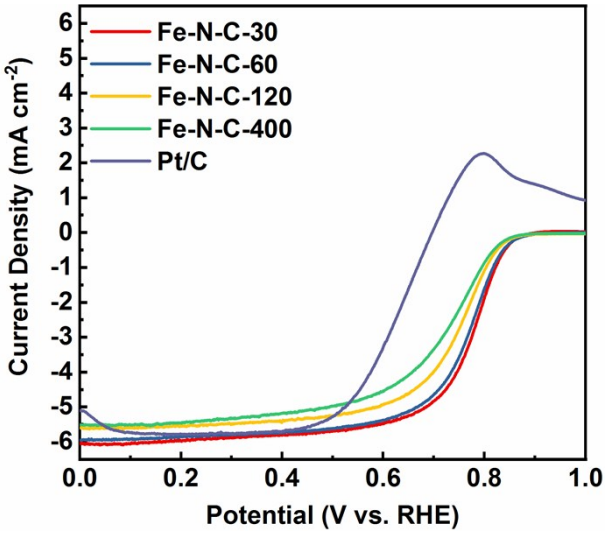

Figure S12. The LSV curves of Fe-N-C-30, Fe-N-C-60, Fe-N-C-120 and Fe-N-C-400 and commercial 20% Pt/C in O_2-saturated 0.1 M $HClO_4$ containing 0.5 M methanol.

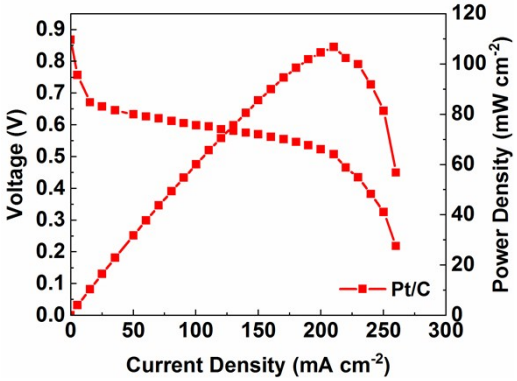

Figure S13. Polarization and power density curves of commercial Pt/C. Test conditions: cathode loading 2 mg_{Pt} cm^{-2} for commercial 60% Pt/C, anode loading 6 mg cm^{-2} for PtRu black, Nafion® 212 membrane, 4 cm^2 electrode, 80 °C, 0.5 M methanol at a flow rate of 1 ml min^{-1}, O_2 at a flow rate of 100 ml min^{-1}.

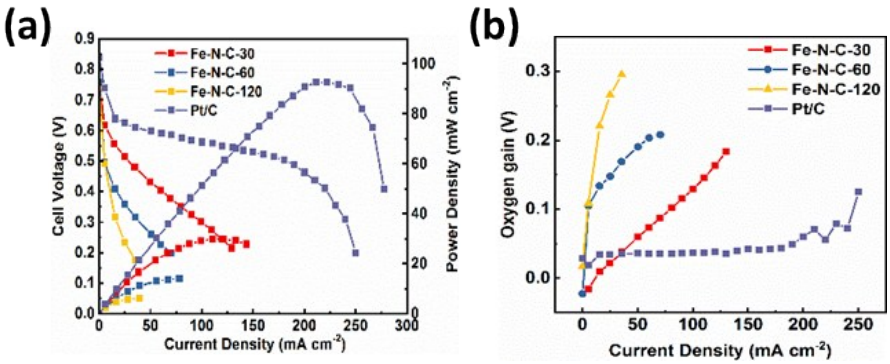

Figure S14. (a) DMFC single cell performance of different cathode catalysts in air and (b) oxygen again results.

2. Table S1-S4

Table S1. Synthesis conditions of ZIF-8 along with their particle sizes.

Sample	CH_3OH: Zn^{2+}	Average size (nm)
ZIF-8-30	1000	31.03
ZIF-8-60	500	60.15
ZIF-8-120	250	122.20
ZIF-8-400	125	420.25

Table S2. Summary of the content of different types of N in the high resolution N1s spectra of Fe-N-C with different sizes.

	Pyridinic N %	Pyrrolic N 399.9 eV %	Graphitic N 401.1 eV %
Fe-N-C-30	54.35	28.15	17.50
Fe-N-C-60	52.38	27.92	19.70
Fe-N-C-120	52.74	28.89	18.37
Fe-N-C-400	52.61	27.87	19.52

Table S3. Summary of BET surface area, micropore surface area, mesopore surface area and the percentage of mesopore of ZIF-8 and Fe-N-C with different sizes.

	Surface Area ($m^2 g^{-1}$)	**Micropore Area ($m^2 g^{-1}$)**	**Mseopore Area ($m^2 g^{-1}$)**	**Percentage of Mesopore**
ZIF-8-30	1327	1092	235	17.7%
ZIF-8-60	1520	1388	132	8.7%
ZIF-8-120	1716	1602	114	6.6%
ZIF-8-400	1932	1885	47	2.43%
Fe-N-C-30	681	467	214	31.4%
Fe-N-C-60	691	522	169	24.4%
Fe-N-C-120	714	550	164	23.0%
Fe-N-C-400	771	624	147	19.1%

Table S4. Summary of E_{onset}, $E_{1/2}$ and j_l of Fe-N-C with different sizes.

Sample	E_{onset} (V)	$E_{1/2}$ (V)	j_l (mA cm^{-2})
Fe-N-C-30	0.874	0.78	5.953
Fe-N-C-60	0.875	0.765	5.787
Fe-N-C-120	0.88	0.742	5.427
Fe-N-C-400	0.876	0.718	5.343